Recent advances in Spectroscopic Investigations on Ionic Liquid/Electrode Interfaces

Kenta Motobayashi,[1,]* and *Masatoshi Osawa*[2]

[1]Department of Physical Science and Engineering, Graduate School of Engineering, Nagoya Institute of Technology, Nagoya, 466-8555, Japan

[2]Institute for Catalysis, Hokkaido University, Sapporo, 001-0021, Japan

AUTHOR INFORMATION

Corresponding Author

kmotobayashi@nitech.ac.jp

ABSTRACT:

Potential applications of room temperature ionic liquids (RTILs) for electrochemical energy devices motivate a better fundamental understanding of electrochemical interfaces of RTILs. Potential-dependent structural changes of RTILs/electrode interfaces and elementary processes of electrode kinetics must be elucidated. Interface-sensitive spectroscopic techniques, powerful probes for analyzing structures and dynamics of interfaces, have revealed hysteretic adsorption/desorption of ions on electrodes, interplay between the interfacial structures and reactions, and dynamics of intermediate species. Here we briefly review selected publications reported over the past 3 years related to molecular-scale investigations on electrochemical interfaces of RTILs with the use of spectroscopic techniques.

KEYWORDS

spectroelectrochemistry, solid/liquid interface, ionic liquids, electrical double layer

1. Introduction

Room temperature ionic liquids (RTILs) are liquid salts at ambient temperature composed purely of cations and anions. The unique properties of RTILs, including high thermal stability, wide electrochemical windows, and high ionic conductivity, make them attractive substances for fundamental and applied research, particularly for applications to electrochemical devices such as batteries or capacitors [1-5]. The central part of such applications is the RTIL/electrode interface where electrochemical reactions occur; hence, a molecular scale description of the interface is essential for improving devices. RTILs, composed purely of charged species, are expected to show much different interfacial structures from the conventional electrochemical double layer explained by Gouy-Chapman-Stern theory for dilute electrolyte solutions [6-8], and then the multiple alternating layers of cations and anions have been revealed by X-ray reflectometry (XR) [9], surface force apparatus (SFA) [10, 11], and atomic force microscopy (AFM) [12] as well as various theoretical works [13-15].

For fundamental understanding of the ionic multilayer structure, in-situ microscopic and spectroscopic techniques combined with electrochemistry have been applied. AFM has revealed the thickness of multilayers and the vertical distribution of ions [16-18], while scanning tunneling microscopy (STM) revealed the lateral order of ions [19-21] as well as potential-dependent morphology of the electrode [22, 23] as recently reviewed [24, 25]. Various in-situ vibrational spectroscopies have been applied, such as sum frequency generation (SFG) [26-30], surface-enhanced Raman spectroscopy (SERS) [31, 32], shell-isolated nanoparticle enhanced Raman spectroscopy (SHINERS) [33], and surface-enhanced infrared absorption spectroscopy (SEIRAS) [34-40]. Measurements with these techniques have revealed the adsorption of cations on negatively charged electrode surfaces and the replacement with the anions on positively charged surfaces

accompanied by a potential-dependent reorientation of the ions. A hysteretic potential-dependence of these interfacial restructuring has been also shown. In addition, potential-dependent transitions of the interfacial structures have been predicted theoretically (lateral ordered-disordered transitions [41], and horizontal structural transitions between monolayer, multilayer, bulk-like, and "crowded" structures [42-44]).

Ionic multilayers are nowadays accepted to be a common interfacial structure for various RTILs [45]. Over the past 3 years, details of the potential-triggered restructuring of the interface depending on constituent ions, electrode materials, and temperature have been studied to understand the mechanism of the formation and hysteretic behavior of ionic multilayers. Furthermore, in-situ spectroscopic observations of electrochemical reactions at RTIL/electrode interfaces have been performed to elucidate the interplay between interfacial structures and reactions, and dynamics of intermediate species, which are difficult to observe by scanning probe techniques. Herein, we present a brief overview on recent achievements in spectroscopic investigations of RTIL/electrode interfaces to highlight significant advancements in fundamental understanding of the interfaces.

2. Mechanistic studies on potential-dependent behavior of interfacial structures

One of the most characteristic features of potential-dependent restructuring of RTIL/electrode interfaces elucidated by in-situ spectroscopic observations is the hysteretic anion-cation exchange in the first ionic layer on electrodes. Hysteretic behaviors were first found in electrochemical impedance spectroscopy (EIS) [46, 47]; however, the origins of the hysteresis could not be clarified by such electrochemical methods alone. Later, Zhou et al. showed the hysteretic adsorption/desorption dynamics of anions in 1-butyl-3-methylimidazolium

trifluoromethanesulfonate [C_4mim][OTf] [29] and 1-butyl-3-methylimidazolium bis(trifluoromethanesulfonyl)amide [C_4mim][TFSA] [30] on Pt with the use of SFG. Concerted adsorption/desorption of cations and anions with hysteresis, and a precedent local ionic concentration change in overlayers during potential scans of [C_4mim][TFSA] on Au have been reported based on SEIRAS measurements [37]. XR studies have also detected similar hysteresis in vertical ion distribution for 1-methyl-3-nonylimidazolium bis(trifluoromethanesulfonyl)amide [C_9mim][TFSA] on epitaxial graphene [48]. After these pioneering works, more systematic investigations have been performed to advance the mechanistic understanding of the hysteretic potential-dependence of the interfacial structures.

In contrast to AFM studies [16, 18], no systematic comparison between various kinds of RTILs or electrode materials had been reported in spectroscopic studies of the interfaces until SEIRAS studies of various RTIL/electrode interfaces reported by Motobayashi, Nishi and coworkers [39, 40]. The authors examined RTILs composed of imidazolium-based cations with different alkyl chain lengths combined with different-sized anions including tetrafluoroborate and sulfonylamide ions to elucidate the effects of ion size on the hysteretic interfacial restructuring [40]. As a result, most of the examined RTILs showed hysteretic anion/cation replacement, and their potential dependence suggested that larger-sized ions led to higher activation barriers for the ion replacement in the first layer (Figure 1(a) and (b)). One exception was the case of [C_4mim][BF_4], which showed no hysteretic anion/cation replacement. This is likely because the sufficiently small $[BF_4]^-$ anion can penetrate into the space between cations instead of the anion/cation replacement. From these results, the authors concluded that the steric hindrance of constituent ions significantly contributes to the structural restriction of the first ionic layer which requires an overpotential to be replaced. This work offers that the ion size effect can be utilized for modifying the potential-

dependence of the interfacial structures. The ion size effect has also been highlighted in the SEIRAS study on quaternary ammonium-based RTILs on Au [39], where the penetration of the neutral alkyl chain of the cations into the space between anions in the first ionic layer at positive potentials was discussed. It has been found that the penetration occurs only when the anion is small (space between the anions is sufficiently large) and the cation alkyl chain length is sufficiently long. It has been suggested that the neutral alkyl chains act as space-filling moieties, which probably have a loose structure that can be replaced by additional redox species coming from the bulk RTIL much more easily than the charged parts of the RTIL ions forming the first ionic layer. Although it has yet to be verified, such an assumption on ion-size effects opens the new way to control the reactivity of RTIL/electrode interfaces.

XR is the method that revealed the multi-layered structure of RTILs on solid surfaces in early times of the research, and recently combined with electrochemical techniques to investigate the structure and dynamics of RTILs on Si [49], boron doped diamond [50], and graphite [48, 51] electrode surfaces. X-ray scattering studies have also been performed for those on Si [52] and Au [53]. Among these, recently the origin of the hysteretic potential-dependence of the interfacial structure has been discussed through a temperature-dependent XR study of [C_9mim][TFSA] on an epitaxial graphene electrode (Figure 1(c)) [51]. The hysteresis was observed at all examined temperatures (25-100 ˚C, Figure 1(d)). The overpotential required for the structural transition showed negligible temperature dependence, whereas broader potential variation was required for completing the transition at higher temperatures as shown in Figure 1(e). The authors explained these results on the basis of a simple bistable model system where two stable states (cation- and anion-adsorbed surfaces) are separated by an energy barrier. The surface could be divided into domains at either state and was described as “a linear combination of contribution from individual

domains". The energy barrier for the structural transition can be inhomogeneous for these domains due to some possible factors such as inhomogeneity in charge within the graphene layers or that in ion-surface interactions. This simple model suggests that the necessity of broader potential variation for the structural transitions at higher temperatures originate from greater inhomogeneity owing to significant thermal fluctuation. The temperature-dependent XR experiments make this simple inhomogeneous domain structure model plausible, which is also applicable to explain the broad potential ranges for structural transition appeared in SFG [29, 30] and SEIRAS[37, 39, 40].

Various analysis methods, including EIS, SFG, SEIRAS, and XR, have detected the hysteresis for different combinations of RTILs and electrode materials. These studies have led to the conclusion that this hysteretic behavior is a general characteristic of RTIL/electrode interfaces with few exceptions. Recent systematic studies revealed the ion-size effects and temperature effects on potential-dependent restructuring of the electrochemical interfaces of RTILs.

3. Interplay between interfacial structure of RTILs and electrochemical reactions

The ionic multilayer structure showing hysteretic potential dependence is one of the characteristic features of RTIL/electrode interfaces as reviewed in the previous section. The first ionic layer is so rigid that a certain overpotential or force is required for exchanging adsorbed ions. Therefore, it has been afraid that this rigid first ionic layer might inhibit redox species from adsorption onto electrodes and from subsequent electrochemical reactions [54]. This possibility has been well discussed [55]; however, no direct experimental evidence has been reported until recent in-situ spectroscopic observations of RTIL/electrode interfaces under reaction condition.

RTILs are generally hygroscopic, and complete removal of water content is difficult and costly. Therefore, the potential-dependent behavior of water and its interplay with the interfacial structure

of [C_4mim][TFSA] were investigated by using SEIRAS [38]. What authors found for [C_4mim][TFSA] containing 700 ppm water on Au are: (1) water molecules accumulate at the interface to form a strong H-bond network even at low water contents at which being free from H-bond network in the bulk, (2) the local water concentration is potential-dependent and changes in conjunction with the change in local anion concentration at the interface (Figure 2(a)) as predicted in theoretical studies [56, 57], (3) the initial step of oxidation and reduction of water occurred at the potential where cation/anion replacement starts during potential scans (Figure 2(a) and (b)). It is worth noting that this was the first report suggesting an interplay between electrochemical reactions and the interfacial structure of RTIL/electrode. These findings suggested that the cationic/anionic first layer inhibits the adsorption of water on the electrode, and that the partly disordered interfacial structure resulted from partial cation/anion replacement allow water adsorption and subsequent oxidation/reduction reactions.

RTILs are prospective electrolyte materials for Li ion batteries owing to their wide electrochemical windows. Yamagata et al. reported that the addition of Li salt leads to further extension of the electrochemical window at the negative edge of 1-ethyl-3-methylimidazolium bis(fluorosulfonyl)amide [C_2mim][FSA] on graphite, which was not the case for [C_2mim][TFSA] [58]. To discuss this mechanism in detail, Iwahashi et al. investigated potential responses of adsorption/desorption behavior of $[FSA]^-$ in [C_2mim][FSA] with and without Li^+ on Pt (which showed a similar extension of the electrochemical window) by using SFG [59]. The authors observed potential-dependent SFG signals indicating that $[FSA]^-$ desorbs from the Pt surface when the potential reaches a certain negative value. Addition of Li[FSA] resulted in a negative shift of the desorption potential of the anion (Figure 2(c)). Remaining of $[FSA]^-$ at high negative potentials was attributed to the strong interaction between $[FSA]^-$ and Li^+ which adsorbs onto the negatively

charged electrode surface. The authors concluded that the suppression of cation decomposition and extension of the electrochemical window could be explained by suppression of the adsorption of $[C_2mim]^+$ to the Pt electrode owing to the stable adsorbed layer of $[FSA]^-$ and the Li^+ (Figure 2((d) and (e)).

The CO_2 reduction reaction is another prospective application of RTILs. Their wide electrochemical window enables the CO_2 reduction to occur without any side reactions such as water electrolysis, resulting in a high Faraday efficiency. The overpotential has been reported to be unexpectedly low [60]. To understand the reaction mechanism, in-situ observations of RTIL/electrode interfaces under reaction condition have been performed with various interface-sensitive spectroscopic methods. Among them, Rey et al. investigated the potential-dependent transition of the interfacial structure of $[C_2mim][BF_4]$/Ag during the electrochemical reduction of CO_2 by using nonresonant (NR) SFG measurement [61]. In contrast to resonant SFG signals indicating excitation of molecular vibration, non-resonant signals originates from nonlinear polarizability of the metal electrons, and thus affected by the interfacial restructuring. The authors found that the potential-dependent NR signal intensity showed a parabolic curve with a minimum located at the identical potential with the threshold for CO_2 reduction. The resonant SFG measurement of the Stark shift of the adsorbed CO revealed that the local electric field at the interface was approximately doubled at potentials less positive than this threshold. The above phenomena observed regardless of the presence of CO_2 indicated certain transitions of the interfacial structure (speculated to be an overabundance or higher degree of alignment of cations). Thus, the authors concluded that this structural transition controls the CO_2 reduction process.

4. Detection of intermediate species at RTIL/electrode interfaces

Because the multilayered structure of RTIL/electrode interfaces is much different from the conventional electrochemical double layer found in aqueous solution/electrode interfaces, the mechanisms of electrochemical reactions are expected to be also different. For example, ionic intermediates are expected to be stabilized in the ionic atmosphere in RTILs and elongation of their life time might enhance certain reaction processes (Figure 3(a)) [60]. The adsorption and coordination nature of intermediates have also been discussed [62]. To understand reaction mechanisms, in-situ spectroscopic observations of intermediate species have recently been performed.

The first observation of intermediate species at RTIL/electrode interfaces was performed by Rosen et al. for CO_2-saturated [C_2mim][BF_4] containing 90 mM water on Pt [63], where the SFG band attributed to [CO_2–C_2mim] complex was observed (Figure 3(b)). The reaction mechanism was recently revisited to discuss in more detail in an SFG study on dried [C_2mim][BF_4] on Pt [64]. The authors measured SFG spectra during potential scans and detected absorption bands corresponding to CO_2 antisymmetric stretch mode of [CO_2–C_2mim] complex and CO stretch mode of CO adsorbed on atop sites (Figure 3(c) and (d)). The absorption band of CO observed at positive potentials rapidly decreased its intensity during a cathodic potential sweep, which are accompanied by an intensity increase of the CO_2 complex and a small current peak in cyclic voltammogram (CV). At potentials negative of a certain threshold, an intensity decrease of the CO_2 complex was observed with a simultaneous increase in the reduction current. These results suggest the CO_2 reduction process as follows: first, the [CO_2-C_2mim] complex formed on the surface, and then underwent further reduction to form CO which immediately desorbed from the surface. The produced CO adsorbed on the surface at positive potentials in the subsequent potential cycles, acting as a poisoning species for CO_2 reduction. The authors concluded that the formation of the

[CO_2-C_2mim] intermediate at remarkably high anodic potentials resulted in a low overpotential for CO_2 electroreduction.

Santos et al. reported a SERS study on CO_2 reduction at the [C_4mim][BF_4]/Cu interface [65]. SERS signals of CO with a low frequency were observed at moderately negative potentials, suggesting that CO_2 reduction occurred and that generated CO adsorbed onto the Cu_2O film formed on the electrode at these potentials. At high negative potentials, signs of the Cu_2O film was disappeared and the SERS signal of a C=C double bond and carboxylate moiety were observed, indicating the formation of a carbene and a carbene-CO_2 adduct ([CO_2-C_4mim] complex) as an intermediate, respectively. Thus, different reaction pathways were observed on Cu/Cu_2O and on Cu. These results suggest that Cu/Cu_2O electrodes in RTIL could be used for CO_2 reduction at a lower overpotential.

The O_2 reduction reaction, which is the cathode reaction in lithium-oxygen cells, has also been investigated by using SERS [66]. The SERS measurements of two RTILs on Au revealed the formation and potential-dependent behavior of the superoxide (Figure 3(e)). The potential dependence of the SERS signal intensities of the superoxide well correlated with O_2 reduction current in CV, indicating that superoxide is the intermediate as in the case of aqueous solutions (Figure 3(f)). From a comparison of the behavior and vibrational frequency of the superoxide in the two RTILs, the authors concluded that a more Lewis basic superoxide is generated on the Au electrode when the superoxide is less strongly coordinated by the RTIL cations. Thus, the radical nature of the superoxide intermediate could be controlled by the choice of RTILs.

5. Concluding remarks

Recently interface-sensitive spectroscopy has been widely applied to RTIL/electrode interfaces to investigate interfacial structures and mechanisms of electrochemical reactions. The fruits of the past 3 years can be summarized as follows. (1) Systematic observations of various RTILs on different electrodes with varied parameters resulted in deeper insight into the origins of the hysteretic behavior of the interfacial structures. (2) Combined spectroscopic and electrochemical observations shed light on the interplay between the potential-dependent interfacial structures and reactivity. (3) The behavior of reaction intermediates has been elucidated. Electrochemical reactions are slower in RTILs than in aqueous or organic solvents in general, and this intrinsic nature of RTILs should be improved for wider applications of RTILs. Spectroscopic understanding of the interplay between characteristic interfacial properties of RTILs and electrochemistry opens new avenues to achieve faster and more efficient electrochemical reactions in RTILs.

Meanwhile, partly due to the short history in this research area, accumulated experimental data and insights are not sufficient for total understanding of the structure and reactivity of the electrochemical interfaces of RTILs. The structured domain of RTILs near electrodes is thicker than that of conventional electrolytes; therefore, various analysis methods with different surface selectivity are required, and have been applied as reviewed here. However, application of each method to wide variety of RTILs and electrodes cannot bridge the gaps between the insights from each method. Also problematic is the gap between the insights from the studies using spectroscopies, SPM, and theoretical calculations. For instance, the hysteretic behavior of the interfaces has been reported only in spectroscopic studies. Other way round, no explicit spectroscopic observation has been reported for some transition phenomena on single crystal surfaces observed by SPM [17, 20, 25] and predicted in theoretical works [41-44]. Such variety of gaps should be filled in by further collaborative investigations.

In addition, in-situ observations of electrochemical interfaces based on in-vacuo surface analysis techniques such as X-ray photoelectron spectroscopy (XPS) [67, 68], X-ray absorption spectroscopy (XAS) [69], and photoemission electron microscope (PEEM) [70] have recently been applied and demonstrated their potentials for analysis of the electrochemical interfaces. Applications of these methods with different advantages to an identical RTIL/electrode system will simplify the discussion and enable a better fundamental understanding of electrochemistry in RTILs.

The insights into electrochemical interfaces would also contribute to fundamental understanding of the tribology of RTILs. Nanoscale mechanistic investigation of lubrication phenomena of RTILs have been started by using SPM techniques [71-73] and theoretical calculations [74-76] in which the importance of surface potential/charge has been addressed; however, spectroscopic investigation [77] has been rarely reported that will provide complementary information. Tribology of RTILs is still a frontier research area waiting for the application of surface-selective spectroscopic methods.

Acknowledgment

This work was supported by JSPS KAKENHI Grant Number 25810044 and 15K04683.

References

1. Buzzeo MC, Evans RG, Compton RG: **Non-Haloaluminate Room-Temperature Ionic Liquids in Electrochemistry—A Review**. *ChemPhysChem* 2004, **5**:1106-20.
2. Galiński M, Lewandowski A, Stępniak I: **Ionic liquids as electrolytes**. *Electrochim Acta* 2006, **51**:5567-80.
3. Hapiot P, Lagrost C: **Electrochemical Reactivity in Room-Temperature Ionic Liquids**. *Chem Rev* 2008, **108**:2238-64.
4. Ohno H. Electrochemical aspects of ionic liquids. Hoboken: Wiley; 2011.
5. A. A. J. Torriero, Shiddiky MJA. Electrochemical properties and applications of ionic liquids. New York: Nova; 2011.
6. Kornyshev AA: **Double-Layer in Ionic Liquids: Paradigm Change?** *J Phys Chem B* 2007, **111**:5545-57.
7. Fedorov MV, Kornyshev AA: **Ionic Liquid Near a Charged Wall: Structure and Capacitance of Electrical Double Layer**. *J Phys Chem B* 2008, **112**:11868-72.
8. Oldham KB: **A Gouy-Chapman-Stern model of the double layer at a (metal)/(ionic liquid) interface**. *J Electroanal Chem* 2008, **613**:131-8.
9. Mezger M, Schröder H, Reichert H, Schramm S, Okasinski JS, Schöder S, Honkimäki V, Deutsch M, Ocko BM, Ralston J, Rohwerder M, Stratmann M, Dosch H: **Molecular Layering of Fluorinated Ionic Liquids at a Charged Sapphire (0001) Surface**. *Science* 2008, **322**:424-8.
10. Perkin S, Albrecht T, Klein J: **Layering and shear properties of an ionic liquid, 1-ethyl-3-methylimidazolium ethylsulfate, confined to nano-films between mica surfaces**. *Phys Chem Chem Phys* 2010, **12**:1243-7.
11. Ueno K, Kasuya M, Watanabe M, Mizukami M, Kurihara K: **Resonance shear measurement of nanoconfined ionic liquids**. *Phys Chem Chem Phys* 2010, **12**:4066-71.
12. Atkin R, Warr GG: **Structure in Confined Room-Temperature Ionic Liquids**. *J Phys Chem C* 2007, **111**:5162-8.
13. Fedorov MV, Kornyshev AA: **Ionic Liquids at Electrified Interfaces**. *Chem Rev* 2014, **114**:2978-3036.
14. Kornyshev AA, Qiao R: **Three-Dimensional Double Layers**. *J Phys Chem C* 2014, **118**:18285-90.

15. Dong K, Liu X, Dong H, Zhang X, Zhang S: **Multiscale Studies on Ionic Liquids**. *Chem Rev* 2017, **117**:6636-95.
16. Hayes R, Warr GG, Atkin R: **At the interface: solvation and designing ionic liquids**. *Phys Chem Chem Phys* 2011, **12**:1709-23.
17. Zhong Y-X, Yan J-W, Li M-G, Zhang X, He D-W, Mao B-W: **Resolving Fine Structures of the Electric Double Layer of Electrochemical Interfaces in Ionic Liquids with an AFM Tip Modification Strategy**. *J Am Chem Soc* 2014, **136**:14682-5.
18. Black JM, Zhu M, Zhang P, Unocic RR, Guo D, Okatan MB, Dai S, Cummings PT, Kalinin SV, Feng G, Balke N: **Fundamental aspects of electric double layer force-distance measurements at liquid-solid interfaces using atomic force microscopy**. *Scientific Reports* 2016, **6**:32389.
19. Su Y-Z, Fu Y-C, Yan J-W, Chen Z-B, Mao B-W: **Double Layer of Au(100)/Ionic Liquid Interface and Its Stability in Imidazolium-Based Ionic Liquids**. *Angew Chem Int Ed* 2009, **48**:5148-51.
20. Wen R, Rahn B, Magnussen OM: **Potential-Dependent Adlayer Structure and Dynamics at the Ionic Liquid/Au(111) Interface: A Molecular-Scale In Situ Video-STM Study**. *Angew Chem Int Ed* 2015, **54**:6062-6.
21. Elbourne A, McDonald S, Voïchovsky K, Endres F, Warr GG, Atkin R: **Nanostructure of the Ionic Liquid–Graphite Stern Layer**. *ACS Nano* 2015, **9**:7608-20.
22. Lin LG, Wang Y, Yan JW, Yuan YZ, Xiang J, Mao BW: **An in situ STM study on the long-range surface restructuring of Au(111) in a non-chloroaluminumated ionic liquid**. *Electrochem Commun* 2003, **5**:995-9.
23. Borisenko N, Zein El Abedin S, Endres F: **In Situ STM Investigation of Gold Reconstruction and of Silicon Electrodeposition on Au(111) in the Room Temperature Ionic Liquid 1-Butyl-1-methylpyrrolidinium Bis(trifluoromethylsulfonyl)imide**. *J Phys Chem B* 2006, **110**:6250-6.
24. Fu Y, Rudnev AV: **Scanning probe microscopy of an electrode/ionic liquid interface**. *Current Opinion in Electrochemistry* 2017, **1**:59-65.
25. Yan J-W, Tian Z-Q, Mao B-W: **Molecular-level understanding of electric double layer in ionic liquids**. *Current Opinion in Electrochemistry* 2017, **4**:105-11.

26. Rivera-Rubero S, Baldelli S: **Surface Spectroscopy of Room-temperature Ionic Liquids on a Platinum Electrode: A Sum Frequency Generation Study**. *J Phys Chem B* 2004, **108**:15133-40.
27. Baldelli S: **Surface Structure at the Ionic Liquid-Electrified Metal Interface**. *Acc Chem Res* 2008, **41**:421-31.
28. Bozzini B, Bund A, Busson B, Humbert C, Ispas A, Mele C, Tadjeddine A: **An SFG/DFG investigation of CN^- adsorption at an Au electrode in 1-butyl-1-methyl-pyrrolidinium bis(trifluoromethylsulfonyl) amide ionic liquid**. *Electrochem Commun* 2010, **12**:56-60.
29. Zhou W, Inoue S, Iwahashi T, Kanai K, Seki K, Miyamae T, Kim D, Katayama Y, Ouchi Y: **Double layer structure and adsorption/desorption hysteresis of neat ionic liquid on Pt electrode surface - an in-situ IR-visible sum-frequency generation spectroscopic study**. *Electrochem Commun* 2010, **12**:672-5.
30. Zhou W, Xu Y, Ouchi Y: **Hysteresis Effects in the In Situ SFG and Differential Capacitance Measurements on Metal Electrode/Ionic Liquids Interface**. *ECS Transactions* 2013, **50**:339-48.
31. Santos VO, Alves MB, Carvalho MS, Suarez PAZ, Rubim JC: **Surface-Enhanced Raman Scattering at the Silver Electrode/Ionic Liquid ($BMIPF_6$) Interface**. *J Phys Chem B* 2006, **110**:20379-85.
32. Yuan Y-X, Niu T-C, Xu M-M, Yao J-L, Gu R-A: **Probing the adsorption of methylimidazole at ionic liquids/Cu electrode interface by surface-enhanced Raman scattering spectroscopy**. *J Raman Spectrosc* 2009, **41**:516-23.
33. Zhang M, Yu L-J, Huang Y-F, Yan J-W, Liu G-K, Wu D-Y, Tian Z-Q, Mao B-W: **Extending the shell-isolated nanoparticle-enhanced Raman spectroscopy approach to interfacial ionic liquids at single crystal electrode surfaces**. *Chem Commun* 2014, **50**:14740-3.
34. Nanbu N, Kato T, Sasaki Y, Kitamura F: **In Situ SEIRAS Study of Room-temperature Ionic Liquid | Gold Electrode Interphase**. *Electrochemistry* 2005, **73**:610-3.
35. Romann T, Oll O, Pikma P, Lust E: **Abnormal infrared effects on bismuth thin film–MImBF4 ionic liquid interface**. *Electrochem Commun* 2012, **23**:118-21.
36. Yang Y-Y, Zhang L-N, Osawa M, Cai W-B: **Surface-Enhanced Infrared Spectroscopic Study of a CO-Covered Pt Electrode in Room-Temperature Ionic Liquid**. *J Phys Chem Lett* 2013, **4**:1582-6.

37. Motobayashi K, Minami K, Nishi N, Sakka T, Osawa M: **Hysteresis of Potential-Dependent Changes in Ion Density and Structure of an Ionic Liquid on a Gold Electrode: In Situ Observation by Surface-Enhanced Infrared Absorption Spectroscopy**. *J Phys Chem Lett* 2013, **4**:3110-4.
38. Motobayashi K, Osawa M: **Potential-dependent condensation of Water at the Interface between ionic liquid [BMIM][TFSA] and an Au electrode**. *Electrochem Commun* 2016, **65**:14-7.
39. Nishi N, Minami K, Motobayashi K, Osawa M, Sakka T: **Interfacial Structure at the Quaternary Ammonium-Based Ionic Liquids|Gold Electrode Interface Probed by Surface-Enhanced Infrared Absorption Spectroscopy: Anion Dependence of the Cationic Behavior**. *J Phys Chem C* 2017, **121**:1658-66.
40. Motobayashi K, Nishi N, Inoue Y, Minami K, Sakka T, Osawa M: **Potential-induced restructuring dynamics of ionic liquids on a gold electrode: Steric effect of constituent ions studied by surface-enhanced infrared absorption spectroscopy**. *J Electroanal Chem* 2017, **800**:126-33.
41. Merlet C, Limmer DT, Salanne M, van Roij R, Madden PA, Chandler D, Rotenberg B: **The Electric Double Layer Has a Life of Its Own**. *J Phys Chem C* 2014, **118**:18291-8.
42. Kirchner K, Kirchner T, Ivaništšev V, Fedorov MV: **Electrical double layer in ionic liquids: Structural transitions from multilayer to monolayer structure at the interface**. *Electrochim Acta* 2013, **110**:762-71.
43. Ivaništšev V, O'Connor S, Fedorov MV: **Poly(a)morphic portrait of the electrical double layer in ionic liquids**. *Electrochem Commun* 2014, **48**:61-4.
44. Ivaništšev V, Kirchner K, Kirchner T, Fedorov MV: **Restructuring of the electrical double layer in ionic liquids upon charging**. *J Phys: Condens Matter* 2015, **27**:102101.
45. Hayes R, Warr GG, Atkin R: **Structure and Nanostructure in Ionic Liquids**. *Chem Rev* 2015, **115**:6357-426.
46. Drüschler M, Huber B, Passerini S, Roling B: **Hysteresis Effects in the Potential-Dependent Double Layer Capacitance of Room Temperature Ionic Liquids at a Polycrystalline Platinum Interface**. *J Phys Chem C* 2010, **114**:3614-7.

47. Drüschler M, Huber B, Roling B: **On Capacitive Processes at the Interface between 1-Ethyl-3-methylimidazolium tris(pentafluoroethyl)trifluorophosphate and Au(111)**. *J Phys Chem C* 2011, **115**:6802-8.
48. Uysal A, Zhou H, Feng G, Lee SS, Li S, Fenter P, Cummings PT, Fulvio PF, Dai S, McDonough JK, Gogotsi Y: **Structural Origins of Potential Dependent Hysteresis at the Electrified Graphene/Ionic Liquid Interface**. *J Phys Chem C* 2014, **118**:569-74.
49. Chu M, Miller M, Douglas T, Dutta P: **Ultraslow Dynamics at a Charged Silicon–Ionic Liquid Interface Revealed by X-ray Reflectivity**. *J Phys Chem C* 2017, **121**:3841-5.
50. Reichert P, Kjaer KS, Brandt van Driel T, Mars J, Ochsmann JW, Pontoni D, Deutsch M, Nielsen MM, Mezger M: **Molecular scale structure and dynamics at an ionic liquid/electrode interface**. *Faraday Discuss* 2018, **206**:141-57.
51. Uysal A, Zhou H, Feng G, Lee SS, Li S, Cummings PT, Fulvio PF, Dai S, McDonough JK, Gogotsi Y, Fenter P: **Interfacial ionic 'liquids': connecting static and dynamic structures**. *J Phys: Condens Matter* 2015, **27**:032101.
52. Chu M, Miller M, Dutta P: **Crowding and Anomalous Capacitance at an Electrode–Ionic Liquid Interface Observed Using Operando X-ray Scattering**. *ACS Cent Sci* 2016, **2**:175-80.
53. Tamura K, Nishihata Y: **Study on the Behavior of Halide Ions on the Au(111) Electrode Surface in Ionic Liquids Using Surface X-ray Scattering**. *J Phys Chem C* 2016, **120**:15691-7.
54. Yokota Y, Harada T, Fukui K-i: **Direct observation of layered structures at ionic liquid/solid interfaces by using frequency-modulation atomic force microscopy**. *Chem Commun* 2010, **46**:8627-9.
55. Endres F, Höfft O, Borisenko N, Gasparotto LH, Prowald A, Al-Salman R, Carstens T, Atkin R, Bund A, Zein El Abedin S: **Do solvation layers of ionic liquids influence electrochemical reactions?** *Phys Chem Chem Phys* 2010, **12**:1724-32.
56. Feng G, Jiang X, Qiao R, Kornyshev AA: **Water in Ionic Liquids at Electrified Interfaces: The Anatomy of Electrosorption**. *ACS Nano* 2014, **8**:11685-94.
57. Zhang F, Fang C, Qiao R: **Effects of Water on Mica–Ionic Liquid Interfaces**. *J Phys Chem C* 2018, **122**:9035-45.

58. Yamagata M, Nishigaki N, Nishishita S, Matsui Y, Sugimoto T, Kikuta M, Higashizaki T, Kono M, Ishikawa M: **Charge–discharge behavior of graphite negative electrodes in bis(fluorosulfonyl)imide-based ionic liquid and structural aspects of their electrode/electrolyte interfaces**. *Electrochim Acta* 2013, **110**:181-90.
59. Iwahashi T, Miwa Y, Zhou W, Sakai Y, Yamagata M, Ishikawa M, Kim D, Ouchi Y: **IV-SFG studies on the effect of Li+ in extending the electrochemical window at the Pt |[C$_2$mim][FSA] interface**. *Electrochem Commun* 2016, **72**:54-8.
60. Rosen BA, Salehi-Khojin A, Thorson MR, Zhu W, Whipple DT, Kenis PJA, Masel RI: **Ionic Liquid-Mediated Selective Conversion of CO_2 to CO at Low Overpotentials**. *Science* 2011, **334**:643-4.
61. García Rey N, Dlott DD: **Structural Transition in an Ionic Liquid Controls CO_2 Electrochemical Reduction**. *J Phys Chem C* 2015, **119**:20892-9.
62. Lau GPS, Schreier M, Vasilyev D, Scopelliti R, Grätzel M, Dyson PJ: **New Insights Into the Role of Imidazolium-Based Promoters for the Electroreduction of CO_2 on a Silver Electrode**. *J Am Chem Soc* 2016, **138**:7820-3.
63. Rosen BA, Haan JL, Mukherjee P, Braunschweig B, Zhu W, Salehi-Khojin A, Dlott DD, Masel RI: **In Situ Spectroscopic Examination of a Low Overpotential Pathway for Carbon Dioxide Conversion to Carbon Monoxide**. *J Phys Chem C* 2012, **116**:15307-12.
64. Braunschweig B, Mukherjee P, Haan JL, Dlott DD: **Vibrational sum-frequency generation study of the CO_2 electrochemical reduction at Pt/EMIM-BF_4 solid/liquid interfaces**. *J Electroanal Chem* 2017, **800**:114-25.
65. Santos VO, Leite IR, Brolo AG, Rubim JC: **The electrochemical reduction of CO2 on a copper electrode in 1-n-butyl-3-methyl imidazolium tetrafluoroborate (BMI.BF_4) monitored by surface-enhanced Raman scattering (SERS)**. *J Raman Spectrosc* 2016, **47**:674-80.
66. Radjenovic PM, Hardwick LJ: **Time-resolved SERS study of the oxygen reduction reaction in ionic liquid electrolytes for non-aqueous lithium-oxygen cells**. *Faraday Discuss* 2018, **206**:379-92.
67. Camci MT, Aydogan P, Ulgut B, Kocabas C, Suzer S: **XPS enables visualization of electrode potential screening in an ionic liquid medium with temporal- and lateral-resolution**. *Phys Chem Chem Phys* 2016, **18**:28434-40.

68. Aydogan Gokturk P, Donmez SE, Ulgut B, Turkmen YE, Suzer S: **Optical and XPS evidence for the electrochemical generation of an N-heterocyclic carbene and its CS2 adduct from the ionic liquid [bmim][PF_6]**. *New J Chem* 2017, **41**:10299-304.
69. Medina-Ramos J, Lee SS, Fister TT, Hubaud AA, Sacci RL, Mullins DR, DiMeglio JL, Pupillo RC, Velardo SM, Lutterman DA, Rosenthal J, Fenter P: **Structural Dynamics and Evolution of Bismuth Electrodes during Electrochemical Reduction of CO_2 in Imidazolium-Based Ionic Liquid Solutions**. *ACS Catalysis* 2017, **7**:7285-95.
70. Sitaputra W, Stacchiola D, Wishart JF, Wang F, Sadowski JT: **In Situ Probing of Ion Ordering at an Electrified Ionic Liquid/Au Interface**. *Adv Mater* 2017, **29**:1606357.
71. Sweeney J, Hausen F, Hayes R, Webber GB, Endres F, Rutland MW, Bennewitz R, Atkin R: **Control of Nanoscale Friction on Gold in an Ionic Liquid by a Potential-Dependent Ionic Lubricant Layer**. *Phys Rev Lett* 2012, **109**:155502.
72. Li H, Rutland MW, Atkin R: **Ionic liquid lubrication: influence of ion structure, surface potential and sliding velocity**. *Phys Chem Chem Phys* 2013, **15**:14616-23.
73. Li H, Wood RJ, Rutland MW, Atkin R: **An ionic liquid lubricant enables superlubricity to be "switched on" in situ using an electrical potential**. *Chem Commun* 2014, **50**:4368-70.
74. Fajardo OY, Bresme F, Kornyshev AA, Urbakh M: **Electrotunable Lubricity with Ionic Liquid Nanoscale Films**. *Scientific Reports* 2015, **5**:7698.
75. Fajardo OY, Bresme F, Kornyshev AA, Urbakh M: **Electrotunable Friction with Ionic Liquid Lubricants: How Important Is the Molecular Structure of the Ions?** *J Phys Chem Lett* 2015, **6**:3998-4004.
76. Pivnic K, Fajardo OY, Bresme F, Kornyshev AA, Urbakh M: **Mechanisms of Electrotunable Friction in Friction Force Microscopy Experiments with Ionic Liquids**. *J Phys Chem C* 2018, **122**:5004-12.
77. Watanabe S, Nakano M, Miyake K, Tsuboi R, Sasaki S: **Effect of Molecular Orientation Angle of Imidazolium Ring on Frictional Properties of Imidazolium-Based Ionic Liquid**. *Langmuir* 2014, **30**:8078-84.

·· Papers of outstanding interest.

38. First report on interplay between interfacial structures of RTILs and electrochemical reactions.

39. First spectroscopic investigation on systematic ion size dependence of interfacial structure of RTILs.

40. First report on spectroscopic investigation on systematic ion size dependence of hysteretic potential-response of interfacial structures of RTILs.

51. First report on temperature dependence of hysteretic potential-response of RTIL interface.

59. Explains the origin of the extention of the electrochemical window induced by addition of Li salt from interfacial structure of RTILs.

64. Systematic invesitgation elucidating roles of surface species in CO_2 reduction reaction at the RTIL/Ag interface.

65. Observation of two different reduction processes of CO_2 on Cu and Cu/Cu_2O with different overpotentials

66. In-situ obseravtion of intermediates in O_2 reduction reaction in RTILs.

· Papers of special interest.

9. First spectroscopic observation of multi-layered interfacial structure of RTILs on a solid surface.

26. First report on surface-sensitive vibrational spectroscopy of an electrochemical interface of a RTIL.

29. First report on spectroscopic observations of hysteretic potential dependence of a RTIL/electrode interface.

60. Observation suggesting an interplay between interfacial structure of RTILs and CO_2 reduction reaction.

61. First observation of unexpectedly low overpotential of CO_2 reduction reaction on an Ag electrode.

63. First spectroscopic observation of an intermediates of an electrochemical reaction in RTILs.

Figure captions

Fig. 1. (a), (b) SEIRA band intensities of [C_4mim][TFSA]/Au (a) and [C_4mim][NFSA]/Au (b) as a function of electrode potential recorded during the potential scans at 2 mV/s. Adopted from ref. [40]. (c) Schematic representation of the XR scattering geometry from the RTIL/graphite interface under electrochemical control and simplified models of the interfacial structures. (d) Potential-dependent XR data (symbols) with fit lines calculated according to the simple bistable model. (e) Temperature dependence of the fitting parameters: transition width σ, the center of the hysteresis curve V_0, and the hysteresis magnitude ΔV as indicated by the separation between the cathodic and anodic scan curves. Adopted from ref. [51].

Fig. 2. Fig. 2. (a) SEIRA band intensities of [C_4mim][TFSA]/Au as a function of electrode potential recorded during the potential scans at 2 mV/s in dry (water content c_w < 1 ppm) and humid (c_w = 700 ppm) condition. (b) CVs simultaneously measured with SEIRAS in dry and humid [C_4mim][TFSA]. Inset is the schematics of potential dependent change of the interfacial structure. Adopted from ref. [38]. (c) SFG band intensity of SO_2 in-phase asymmetric stretch mode of [FSA] anion in the SFG spectra of the [C_2mim][FSA]/Pt as a function of potential with and without Li^+. (d), (e) Schematic illustrations of applied potential dependence of interfacial structure of [C_2mim][FSA]/Pt without Li^+ (d) and with Li^+ (e). Adopted from ref. [59].

Fig. 3. (a) Schematic showing of how the free energy of the system changes the CO_2 reduction reaction in molecular solvents (solid line) or [C_2mim][BF_4] (dashed line). (b) Schematics of the proposed reaction mechanism of CO_2 reduction in [C_2mim][BF_4]/Ag. Adopted from ref. [63]. (c), (d) SFG spectra of CO and interfacial CO_2 at [C_2mim][BF_4]/Pt interface recorded during the first (c) and the 15^{th} (d) potential cycle at 5 mV/s where electrochemical reduction of CO_2 occurs. Adopted from ref. [64]. (e) SERS spectra of oxygen saturated triethylsulfonium

bis(trifluoromethanesulfonyl)imide [TES][TFSA]/Au at various potentials. (f) Top, CV of oxygenated [TES][TFSA] at 100 mV/s with normal ORR/OER cycle (dashed line) and extended reduction cycle (blue line). Top right inset shows potential region where superoxide bands first appear with small current response. Bottom, frequency and intensity of SERS signals of O-O and O-Au stretch modes as a function of potential. Adopted from ref. [66].

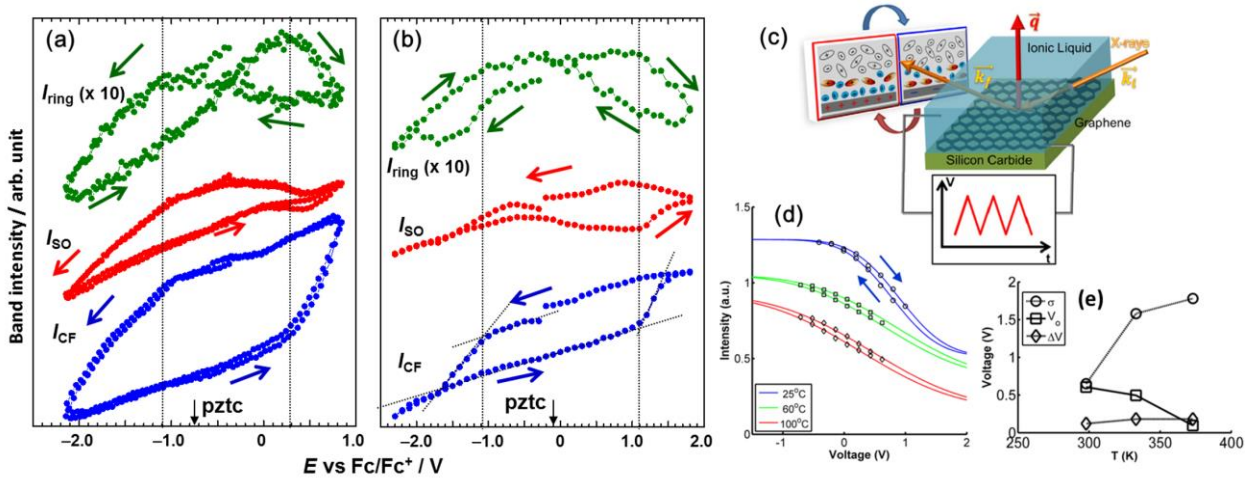

Figure 1

Motobayashi et al.

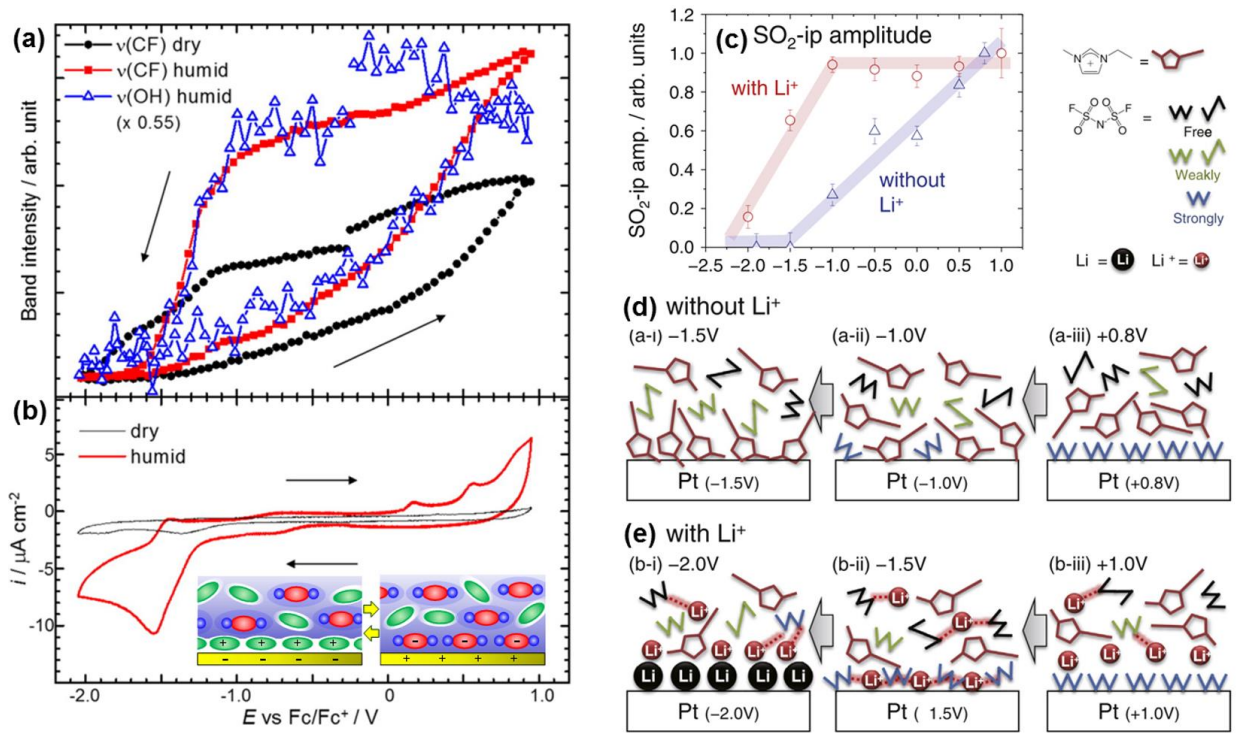

Figure 2

Motobayashi et al.

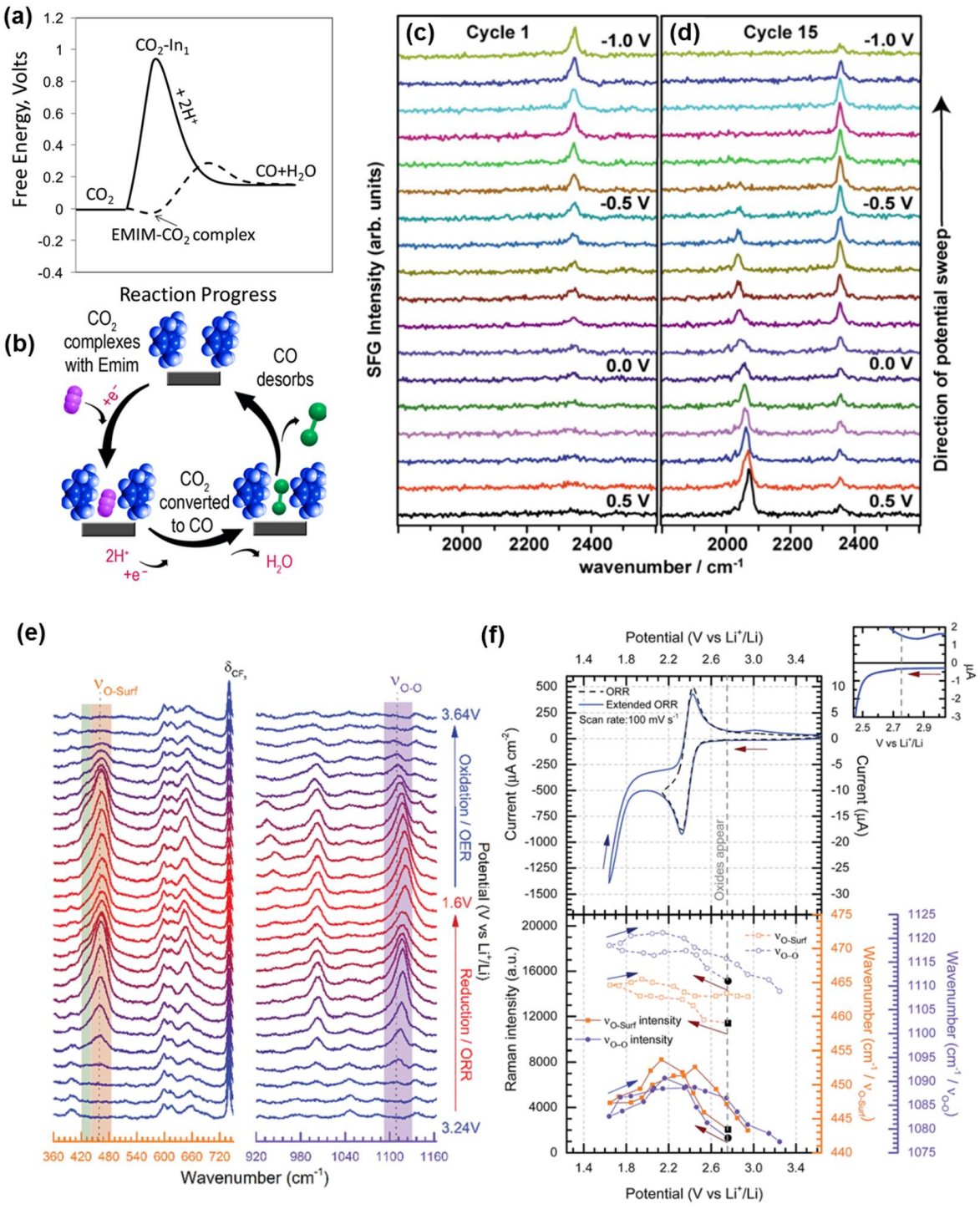

Figure 3

Motobayashi et al.